J|A|C|S ARTICLES

Published on Web 05/22/2009

Aromatic Amino Acids as Stepping Stones in Charge Transfer in Respiratory Complex I: An Unusual Mechanism Deduced from Atomistic Theory and Bioinformatics

Christian Wittekindt,[†] Michael Schwarz,[†] Thorsten Friedrich,[‡] and Thorsten Koslowski*,[†]

Institut für Physikalische Chemie, Universität Freiburg, Albertstrasse 23a, D-79104 Freiburg im Breisgau, Germany, and Institut für Organische Chemie und Biochemie, Universität Freiburg, Albertstrasse 21, D-79104 Freiburg im Breisgau, Germany

Received January 21, 2009; E-mail: koslowsk@uni-freiburg.de

Abstract: With the help of a recent X-ray structure analysis of the hydrophilic part of the bacterial respiratory complex I, we present a theoretical and numerical study of the charge transfer properties of this protein. Our analysis is based upon an atomistic electronic structure model that accounts for the formation of chemical bonds, spin polarization on transition metal atoms, and solvent polarization effects. Solving this model at the Hartree−Fock mean-field level, we are able to access the energy parameters required to compute charge transfer rates, making use of Marcus's theory of nonadiabatic electron transfer. Besides iron−sulfur clusters, aromatic amino acids are identified as essential centers of localization that participate in the electron transfer process. This novel perspective of charge transfer in complex I is substantiated by a multiple sequence analysis of a broad spectrum of genomes, revealing that the amino acids identified as stepping stones in the electron transfer chain are conserved during the evolution of complex I.

1. Introduction

Proteins containing aggregates of iron and sulfur are ubiquitous in nature,[1−3] and their Fe/S cluster cofactors are believed to be among the oldest catalytic groups to have appeared in the tree of life.[4] As iron easily undergoes a change of its formal oxidation state from +2 to +3, Fe/S clusters participate in many redox and electron transfer reactions, in particular in photosynthetic and respiratory electron transfer. In addition, they are essential for the functionality of individual enzymes like aconitase,[5] biotin synthase,[6] pyruvate-formiate lyase,[7] and lysine-amino mutase,[8] and they are likely to play an important role in the expression of genes in bacteria.[9] The most familiar representatives of Fe/S clusters are the planar centers [2Fe-2S], e.g., of the Rieske type, the cubic [4Fe-4S] cluster, the cuboidal [3Fe-4S] cluster, and three atomic linear arrangements of iron and sulfur.

NADH:ubiquinone oxidoreducase (EC 1.6.5.3, also referred to as complex I or NDH1) is the first enzyme of both the mitochondrial and the bacterial respiratory chains. It couples the transfer of two electrons from NADH to ubiquinone to the transport of four protons across a membrane and thus contributes to the synthesis of ATP.[10−13] Because of its central role in the respiratory chain, mutations in complex I are linked to many neurodegenerative diseases in humans.[14] For example, the enhanced production of reactive oxygen species due to a malfunction of complex I is discussed to play an important role in Parkinson's disease.[15]

The bacterial complex I consists of 13−15 subunits, which are referred to as NuoA to NuoN and accumulate to a mass of ∼500 kDa. The bacterial complex is often considered as a minimal structural model of an energy-converting NADH: ubiquinone oxidoreductase.[11,16] Electron microscopy has revealed its characteristic L shape with a hydrophobic membrane and a hydrophilic peripheral arm.[11,17,18] The hydrophilic part has been the subject of a recent X-ray structure analysis;[19] it consists of seven subunits which contain all known cofactors: a flavin mononucleotide (FMN) and nine Fe/S clusters, as

[†] Institut für Physikalische Chemie.
[‡] Institut für Organische Chemie und Biochemie.

(1) Arnon, D. I.; Whatley, F. R.; Allen, M. B. *Nature* **1957**, *180*, 182–185.
(2) Mortenson, L. E.; Valentine, R. C.; Carnahan, J. E. *Biochem. Biophys. Res. Commun.* **1962**, *7*, 448.
(3) Beinert, H.; Sands, R. H. *Biochem. Biophys. Res. Commun.* **1960**, *3*, 41.
(4) Huber, C.; Wächtershäuser, G. *Science* **1998**, *281*, 670–672.
(5) Werst, M. M.; Kennedy, M. C.; Houseman, A. L. P.; Beinert, H.; Hoffmann, B. M. *Biochemistry* **1990**, *29*, 10533–10540.
(6) Duin, E. C.; Lafferty, M. E.; Crouse, B. R.; Allen, R. M.; Sanyal, I.; Flint, D. H.; Johnson, M. K. *Biochemistry* **1997**, *36*, 11811–11820.
(7) Kulzer, R.; Pils, T.; Kappl, R.; Huttermann, J.; Knappe, J. *J. Biol. Chem.* **1998**, *273*, 4897–4903.
(8) Lieder, K. W.; Booker, S.; Ruzicka, F. J.; Beinert, H.; Reed, G. H.; Frey, P. A. *Biochemistry* **1998**, *37*, 2578–2585.
(9) Hidalgo, E.; Ding, H.; Demple, B. *Trends Biochem. Sci.* **1997**, *22*, 207–210.
(10) Walker, J. E. *Q. Rev. Biophys.* **1992**, *25*, 253–324.
(11) Yagi, T.; Matsuno-Yagi, A. *Biochemistry* **2003**, *42*, 2266–2274.
(12) Weiss, H.; Friedrich, T.; Hofhaus, G.; Preis, D. *Eur. J. Biochem.* **1991**, *197*, 563–576.
(13) Friedrich, T. *J. Bioenerg. Biomembr.* **2001**, *33*, 169–177.
(14) Schapira, A. H. *Biochim. Biophys. Acta* **1998**, *1364*, 261–270.
(15) Dawson, T. M.; Dawson, V. L. *Science* **2003**, *302*, 819–822.
(16) Caroll, J.; Fearnley, I. M.; Skehel, M. J.; Shannon, R. J.; Hirst, J.; Walker, J. E. *J. Biol. Chem.* **2006**, *281*, 117–126.
(17) Gué, V.; Schlitt, A.; Weis, H.; Leonard, K. R.; Friedrich, T. *J. Mol. Biol.* **1998**, *207*, 105–112.
(18) Grigorieff, N. *Curr. Opin. Struct. Biol.* **1999**, *9*, 476–483.
(19) Sazanov, L. A.; Hinchliffe, P. *Science* **2006**, *311*, 1430–1436.

 10.1021/ja900352t CCC: $40.75

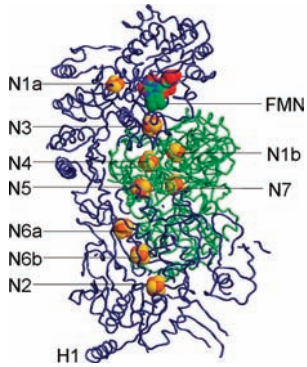

Figure 1. A cartoon representation of complex I from *Thermus thermophilus* (PDB entry: 2FUG) after the X-ray structure.[19] Cofactors are shown as spheres, and the protein as a traced backbone. The NuoG protein subunit is colored in green; all other subunits are colored in blue. For convenience, a small fraction of the protein pointing toward the reader has been removed.

Table 1. Complex I Iron−Sulphur Clusters According to the Nomenclature of Ohnishi[66a]

center	localization	type	midpoint potential (mV)	comment
N1a	NuoE	[2Fe2S]	−330	not in main CT chain
N1b	NuoG	[2Fe2s]	−230	
N2	NuoB	[4Fe4S]	−220	donor to quinone?
N3	NuoF	[4Fe4S]	−270	
N4	NuoG	[4Fe4S]	−270	
N5	NuoG	[4Fe4S]	−250	one His ligand
N6a	NuoI	[4Fe4S]	−270	not yet detected by EPR
N6b	NuoI	[4Fe4S]	−270	not yet detected by EPR
N7	NuoG	[4Fe4S]	−260	not involved in CT

[a] Midpoint potentials refer to *E. coli* and *P. dentrificans* (N5).

depicted and labeled in Figure 1 and listed in Table 1. It is generally proposed that the hydrophilic part is attached to the membrane via an amphipathic helix, labeled as H1 in Figure 1, whereas structural details like the mutual orientation of these entities are still a matter of dispute.[20,21] Within the model presented here, charge transfer rates do not depend on the properties and position of the membrane.

Experimental approaches to measure the total and individual charge transfer rates have been reviewed by Vinogradov.[22] In the most common approach to estimate a rate, the NADH oxidase acitivity of mitochondria or submitochondrial particles is detected. However, in this reaction, complex III and complex IV also participate, and the Fe/S clusters of complex I are predominantly oxidized. The estimated rate of ∼1000 NADH per minute ≡ 30 e^- s^{-1} has thus to be considered as a lower limit to the turnover rate from NADH to oxygen.[22,23] Time-resolved UV/vis spectroscopic studies of the NADH:quinone oxidoreductase activity, on the other hand, suggest a lower limit to the rate of 170 ± 10 s^{-1}.[24,25] Quenching the reaction to the temperature of liquid nitrogen has permitted a time-resolved analysis making use of electron paramagnetic resonance spectroscopy.[26] The EPR signal of the reduced terminal Fe/S cluster N2 was detected after a short time of 90 μs, which sets a lower limit of $\sim 10^4$ s^{-1} for each individual charge transfer step within the electron transfer chain up to that cluster. As no electron transfer to ubiquinone, the final acceptor, was detected here, it is questionable whether the physiological reaction has really been observed. Combining the results of the last two experiments referenced here, we consider it reasonable to have a charge transfer (CT) reaction coefficient k_{CT} =160 s^{-1} as a conservative lower limit of the total transfer rate. Individual steps of the charge transfer chain computed from theoretical models have to fulfill the requirement to be larger than or equal to that estimate.

The knowledge of the spatial arrangement of the cofactors of complex I and their redox potentials (which range from −0.39 to −0.1 V,[27−31] see Table 1) permits a tentative construction of possible electron transfer path, which has been substantiated by a recent phenomenological analysis.[32] Considering the cofactors as the only centers of excess electron localization and assuming an electronic coupling between these entities that exponentially decays with increasing intercluster edge-to-edge donor−acceptor separation R_{DA} as[33]

$$\log_{10} k_{CT} = 15 - 0.6R_{DA} - 3.1\frac{(\Delta G + \lambda)^2}{\lambda} \qquad (1.1)$$

Dutton and co-workers have computed the time-dependent excess electron density along the complex I charge transfer chain.[32] Using the parameters of Moser et al., including a reorganization energy of 0.7 eV, one arrives at rates of 10^6 to 10^7 s^{-1} for all steps except for charge transfer from N5 to N6a, with a rate limiting $k_{CT} \simeq 10^4$ s^{-1}. In addition, Dutton and co-workers conclude that knockout variants of complex I that lack the clusters N1b or N4 not only are functional but CT should be sufficiently fast to be still larger than the total experimental turnover.

In this work, we approach charge transfer through complex I from a more microscopic level, using atoms and their atomic orbitals as the smallest entities of a model of the electronic structure and charge transfer. We focus on charge transfer along the main chain of Fe/S clusters, N3 ⇌ N1b ⇌ N4 ⇌ N5 ⇌ N6a ⇌ N6b ⇌ N2, as N1a and N7 show a considerable distance to this path ($R_{N1\alpha,N3}$ = 22.3 Å, $R_{N4,N7}$ = 20.5 Å) and are usually considered as playing an auxiliary role. FMN was excluded because of the high uncertainty of the driving force for the reaction FMN → N3, and the final acceptor, ubiquinone, is not present in the X-ray structure. Using parameters either stemming from reliable experimental studies (protein and cofactor geometry, driving forces) or from a careful fit to high-level ab initio calculations, a semiempirical model is set up that permits an unbiased treatment of through-space, through-bond, superex-

(20) Morgan, D. J.; Sazanov, L. A. *Biochim. Biophys. Acta* **2008**, *1777*, 711–718.
(21) Clason, T.; Zickermann, V.; Ruiz, T.; Brandt, U.; Rademacher, M. *J. Struct. Biol.* **2008**, 703–710.
(22) Vinogradov, A. D. *Biochim. Biophys. Acta* **1998**, *1364*, 169–185.
(23) Unless otherwise specified, all charge transfer rates correspond to electrons per second.
(24) Stolpe, S.; Friedrich, T. *J. Biol. Chem.* **2004**, *279*, 18377–18383.
(25) Sharpley, M. S.; Shannon, R. I.; Draghi, F.; Hirst, J. *Biochemistry* **2006**, *45*, 241–248.
(26) Verkhovskaya, M. L.; Belevich, N.; Euro, L.; Wilkstr, M.; Verkhovsky, M. I. *Proc. Natl. Acad. Sci. U.S.A.* **2008**, *105*, 2763–3767.
(27) Rasmussen, T.; Scheide, D.; Brors, B.; Kintscher, L.; Weiss, H.; Friedrich, T. *Biochemistry* **2001**, *40*, 6124–6131.
(28) Sled, V. D.; Rudnitzky, N. I.; Hatefi, Y.; Ohnishi, T. *Biochemistry* **1994**, *33*, 10069–10075.
(29) Dutton, P. L.; Moser, C. C.; Sled, V. D.; Daldal, F.; Ohnishi, T. *Biochim. Biophys. Acta* **1998**, *1364*, 245–257.
(30) Ohnishi, T. *Biochim. Biophys. Acta Bioenerg.* **1998**, *1364*, 186–206.
(31) Sazanov, L. A. *Biochemistry* **2007**, *46*, 22752–2288.
(32) Moser, C. C.; Farid, T. A.; Chobot, S. E.; Dutton, P. L. *Biochim. Biophys. Acta* **2006**, *1757*, 1096–1109.
(33) Page, C. C.; Moser, C. C.; Chen, X.; Dutton, P. L. *Nature* **1999**, *402*, 47–52.

Table 2. Center-of-Mass Intercluster Separations R_{DA}, Electronic Tunnel Splittings t_{DA}, and Forward Reaction Coefficients k_{CT} for Charge Transfer between Fe/S Clusters in Complex I Assuming a Through-Space Mechanism[a]

	R_{DA} [Å]	t_{DA} [eV] native PT	t_{DA} [eV] oxidized PT	t_{DA} [eV] oxidized LST	k_{CT} [s^{-1}] oxidized LST
N3 → N1b	14.2	1.0×10^{-7}	1.2×10^{-7}	1.3×10^{-7}	2.2×10^{-2}
N1b → N4	13.9	1.0×10^{-6}	1.6×10^{-6}	1.6×10^{-6}	4.7
N4 → N5	12.2	4.8×10^{-6}	5.3×10^{-6}	5.4×10^{-6}	760
N5 → N6a	16.9	3.1×10^{-9}	3.3×10^{-9}	2.7×10^{-9}	2.2×10^{-4}
N6a → N6b	12.2	7.8×10^{-6}	4.5×10^{-6}	4.2×10^{-6}	720
N6b → N2	14.2	4.3×10^{-7}	5.5×10^{-7}	5.7×10^{-7}	100

[a] The clusters are either fully oxidized or in their presumed native oxidation states; couplings have been computed using the linear synchronous transit (LST) or perturbation theory (PT) approach.

change and hopping transfer within a single unified model. The model and its parameters will be introduced in the next section, followed by the computed Marcus parameters and the emerging charge transfer rates. These findings will be supplemented by multiple sequence alignments of individual complex I subunits to look for the conservation of amino acids identified as central to charge transfer. Finally, we turn to conclusions and place our results in a broader perspective.

2. Model and Methods

To describe the electronic structure and charge transfer properties of large subsections of complex I, we use an empirical Hamiltonian that captures the essential features of the protein and its cofactors. As described below, it is carefully parametrized using ab initio quantum chemical calculations at the density functional theory level. Hence, the model can be expected to combine the advantages of both methods, viz. a fast performance even for large systems consisting of more than 1000 atoms as used here, with the hope not to compromise too seriously on the accuracy. In this manner, we extend a methodology developed by one of the present authors and his co-workers that is suited to describe the energetics of a large variety of charge transfer reactions, with mixed valence bridged organic molecules,[34] Ru-complexed proteins,[35] and DNA hole transfer[36−38] or bionano hybrides[39] as examples.

As essential elements of an electronic structure theory applied to charge transfer in Fe/S cluster proteins, we consider an accurate description of the chemical bond via a tight-binding Hamiltonian $\hat{H}_{tb}$, taking both nearest neighbor and long-range one-electron couplings into account, and a polarization term $\hat{H}_{out}$ that mimics the interaction of an excess charge with the polarizable protein and solvent environment, which is supplemented by an electron−electron interaction H_{ee} that is essential to describe local moment formation and the associated magnetic properties of the Fe/S clusters,

$$\hat{H} = \hat{H}_{tb} + \hat{H}_{out} + \hat{H}_{ee} \qquad (2.1)$$

Details of the electronic structure model and its parametrization are given in the appendix (Supporting Information).

The electronic and magnetic properties of the clusters computed with a combination of the tight-binding and the Hubbard model are in accord with the conventional view on these systems:[3,40−45] oxidized clusters exhibit a net spin of zero, although each iron atom carries a strong local magnetic moment or spin polarization, here computed as $\mu \simeq 3.4$ on each iron. Hence, the predominant magnetic interaction within the clusters is an antiferromagnetic coupling.[46,47] In the cubic Fe_4S_4 clusters, magnetic frustration is observed, and two pairs of neighboring Fe ions exhibit a parallel alignment of their spins. In the case of Fe_4S_4, one to four excess electrons predominantly occupy iron d states, and each electron is delocalized between two iron atoms of the opposite spin. For an odd number of electrons, the net spin gives rise to a doublet, and even numbers give rise to a singlet. Possible exceptions for this view are discussed in refs 48−50.

As will transpire below, the effective electronic couplings t_{DA} between charge donors and acceptors are small compared to all other electronic energy scales. Thus, they permit the computation of charge transfer rates using the diabatic variant of Marcus's theory,

$$k_{CT} = \frac{t_{DA}^2}{\hbar}\sqrt{\frac{\pi}{\lambda k_B T}}\exp\left\{-\frac{(\Delta G - \lambda)^2}{4\lambda k_B T}\right\} \qquad (2.2)$$

As characteristic parameters for each charge transfer step, we have the driving force ΔG, the reorganization energy λ, and the electronic tunnel splitting t_{DA}. For the charge transfer steps of interest, experimental half-step potentials are available, which translate into $\Delta G \simeq 0$, with the exception of the final step, N6b → N2, for which $\Delta G = -0.15$ eV holds (cf. Table 2). Lacking any detailed information about the location of crystal water in the protein or the degree of protonation, we use the experimental ΔG values in connection with eq 2.2 for the computation of charge transfer rates. The tunnel splittings t_{DA} can be computed in two different ways. As the first method, a variational approach can be used. Depending on the initial conditions, SCF computations involving the Hamiltonian A.8 converge into one of several minima because of the strong element of electron−electron attraction faciliated by the outer sphere reaction field contributions. Each of these minima is characterized by a distribution of charges and local magnetic moments. Between these distributions, a linear interpolation can be performed, the so-called linear synchronous transit (LST) approach, giving rise to graphical representations that closely resemble the double well potential of Marcus's theory. As the closest approach of ground and excited state, $2t_{DA}$ can be extracted immediately. The value of the reorganization energy can also read

(34) Utz, N.; Koslowski, T. *Chem. Phys.* **2002**, *282*, 389–397.
(35) Utz, N.; Engel, L.; Friedrich, T.; Koslowski, T. *Z. Phys. Chem.* **2005**, *219*, 1391.
(36) Cramer, T.; Krapf, S.; Koslowski, T. *J. Phys. Chem. B* **2004**, *108*, 11812.
(37) Cramer, T.; Krapf, S.; Koslowski, T. *Phys. Chem. Chem. Phys.* **2004**, *6*, 3160.
(38) Cramer, T.; Steinbrecher, T.; Labahn, A.; Koslowski, T. *Phys. Chem. Chem. Phys.* **2005**, *7*, 4039.
(39) Utz, N.; Koslowski, T. *J. Phys. Chem. B* **2006**, *110*, 9333–9338.
(40) Papaefthymiou, V.; Girerd, J. J.; Moura, I.; Moura, J. J. G.; Münck, E. *J. Am. Chem. Soc.* **1987**, *109*, 4703–4710.
(41) Wang, X.; Niu, S.; Yang, X.; Ibrahim, S. K.; Pickett, C. J.; Ichiye, T.; Wang, L. S. *J. Am. Chem. Soc.* **2003**, *125*, 14072–14081.
(42) Aizman, A.; Case, D. *J. Am. Chem. Soc.* **1982**, *104*, 3269–3279.
(43) Noodleman, L.; Baerends, E. J. *J. Am. Chem. Soc.* **1984**, *106*, 2316–2327.
(44) Noodleman, L.; Case, D. A. *Ad. Inorg. Chem.* **1992**, *38*, 423.
(45) Noodleman, L.; Peng, C. Y.; Case, D. A.; Mouesca, J.-M. *Coord. Chem. Rev.* **1995**, *144*, 199–244.
(46) Zener, C. *Phys. Rev.* **1951**, *82*, 403–405.
(47) Anderson, P. W.; Hasegawa, H. *Phys. Rev.* **1955**, *100*, 675–681.
(48) Achim, C.; Golinelli, M.-P.; Bominaar, E. L.; Meyer, J.; Münck, E. *J. Am. Chem. Soc.* **1996**, *118*, 8168–8169.
(49) Yoo, S. J.; Angove, H. C.; Burgess, B. K.; Hendrich, M. P.; Münck, E. *J. Am. Chem. Soc.* **1999**, *121*, 2534–2545.
(50) Yano, T.; Sklar, J.; Nakamaru-Ogiso, E.; Takahashi, Y.; Yagi, T.; Ohnishi, T. *J. Biol. Chem.* **2003**, *278*, 15514–15522.

directly from the plot, and λ values of 0.7 eV typical of charge transfer processes in proteins can be reproduced by setting the attractive Hubbard parameter equal to 0.57 eV. Alternatively, one may make use of perturbation theory (PT): two molecular orbitals that reside on different clusters and that are sufficiently close in energy interact via their matrix elements and the LCAO-MO coefficients of the unperturbed clusters,

$$t_{DA} = \sum_{ia\in D}\sum_{jb\in A} c_{ia}c_{jb}t_{iajb} \qquad (2.3)$$

3. Results and Discussion

3.1. Through-Space, Through-Bond, and Superexchange Intercluster Charge Transfer Rates. To compute charge transfer rates for through-space processes, all amino acids have been removed from the structure, Fe/S clusters coordinated by either four SCH_3 groups or three SCH_3 groups and an imidazole (cluster N5). In addition, calculations were performed retaining only the coordinating amino acids. The LST approach and PT were used to calculate CT rates between systems consisting of $Fe_2S_2^{2+}$ or $Fe_4S_4^{4+}$ and a single excess electron. PT was also applied to the clusters in their presumed native oxidation state. Using the experimental ΔG values, we obtain the rates listed in Table 2. It is interesting to note that results for different oxidation states are similar, presumably due to the fact that the character of the HOMO is not changed significantly upon reduction. LST and PT give very similar results for the electronic couplings. Three transfer steps (N3 to N1b, N1b to N4, and N5 to N6a) are significantly too small to account for the total experimental turnover of ~160 electrons per second, and even artificially setting the driving forces of the reaction equal to the corresponding reorganization energies does not resolve this mismatch. No major speedup was observed using the Wolfsberg−Helmholtz couplings, as frequently applied within extended Hückel theory,[51,52] instead of their tight-binding counterparts nor by looking for slightly deformed or rotated cluster geometries. Not suprisingly, the process N5→N6a turned out to be the major kinetic bottleneck of CT through the protein for through-space charge transfer.

Within our computations, the charge transfer rates have always been found to depend on the spin states of the two participating clusters. As a consequence, we have calculated k_{CT} for all possible nonequivalent spin configurations. Spin rearrangements at room temperature are much faster ($>10^5$ s^{-1})[53] than the intercluster hopping rates rates estimated from those spin configurations giving rise to the fastest transfers. In turn, the fastest hopping rates have been interpreted as k_{CT}.

Only one pair of clusters is directly linked by a sequence of covalent bonds, viz. N6a and N6b. Here, the two bridges Cys-Ala_3-Cys and Cys-Ala-Glu_2-Cys of the NuoI subunit are candidates for participating in through-bond CT processes. The through-space CT rate of 720 s^{-1} is, however, not increased by considering one of the bridges nor by including both of them in the model calculations.

With their protruding low-energy π orbitals, peptide bonds and aromatic amino acid residues are particularly promising candidates for participating in an electronic superexchange process. For each cluster pair of interest, a cylinder of 10 Å diameter, capped by two hemispheres of the same diameter, was constructed, with the Fe/S cluster centers of mass lying in the centers of the circles that terminate the cylinder. Amino acids located within this object were considered as the geometrical basis of an electronic structure model consisting of covalent tight-binding matrix elements, supplemented by long-range coupling between π and cluster orbitals. Throughout this work, all bonds cut have been saturated by hydrogen atoms. The largest model thus created consists of 1147 atoms. Again, the increase in the rates of the presumed kinetic bottlenecks is small, and we estimate the recomputed rates involving superexchange to be 8.7×10^{-2} s^{-1} (N3 → N1b), 4.6 s^{-1} (N1b → N4), and 2.3×10^{-4} s^{-1} (N5 → N6a). With combined through-space and through-bond contributions to direct coupling and superexchange, we cover all mechanisms used within the widespread phenomenological pathways scheme as introduced by Beratan, Onuchic, and Gray.[54−56] This scheme has found its main field of application in protein charge transfer involving a transition metal complex as a donor,[57,58] a situation for which we note that the variational approach presented here is quantitatively compatible with findings that can be derived from the pathways scheme.[35]

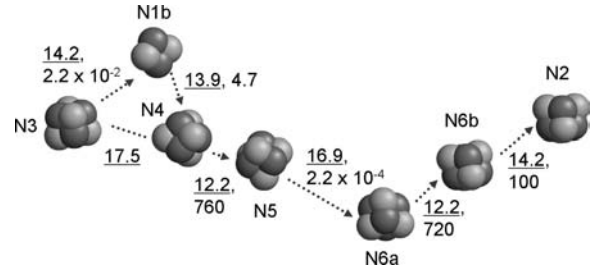

Figure 2. Charge transfer within the main Fe/S cluster electron transport chain in complex I. Cluster atoms are drawn as spheres, and the cluster labels are according to the nomenclature of Ohnishi and co-workers.[66] Center-of-mass intercluster distances (in Å) are underlined and followed by the computed charge transfer rates (in s^{-1}).

Summing up our findings up to this point, neither a properly parametrized through-space charge transfer mechanism between the Fe/S clusters nor a through-bond variant nor a superexchange theory involving a large fraction of the protein can account for the experimentally observed electron turnover. This intermediate conclusion is illustrated with the help of Figure 2, which presents the intercluster distances and the maximum rates achievable by the mechanisms listed above, and Table 2, which supplies similar information from the angle of the effective electronic couplings.

3.2. Hopping Transfer Involving Aromatic Amino Acids. As within a well-parametrized atomistic theory all conventional mechanisms of ground-state charge transfer have seriously failed to reproduce the experimentally observed CT rates, we have considered transient localization of charge carriers on aromatic amino acid side chains as a means of electron transport. This hopping transport hypothesis was motivated as follows. Because of the strong spin pairing energy, excess electrons reside in high

(51) Wolfsberg, M.; Helmholz, L. J. *J. Chem. Phys.* **1952**, *20*, 837–843.
(52) Stuchebrukhov, A. A.; Marcus, R. A. *J. Phys. Chem.* **1995**, *99*, 7581–7590.
(53) Banci, L.; Bertini, I.; Ciurli, S.; Ferretti, S.; Luchinat, C.; Piccioli, M. *Biochemistry* **1993**, *32*, 9387–9397.
(54) Pande, V. S.; Onuchic, J. N. *Phys. Rev. Lett.* **1997**, *78*, 146–149.
(55) Beratan, D. N.; Onuchic, J. N.; Winkler, J. R.; Gray, H. B. *Science* **1992**, *258*, 1740–1741.
(56) Onuchic, J. N.; Beratan, D. N.; Winkler, J. R.; Gray, H. B. *J. Biomol. Struct.* **1992**, *21*, 349–377.
(57) DeJonge, N.; Rau, H. K.; Haehnel, W. *Z. Phys. Chem.* **1999**, *213*, 175–180.
(58) Discher, B. M.; Koder, R. L.; Moser, C. C.; Dutton, P. L. *Curr. Opin. Chem. Biol.* **2003**, *7*, 741–748.

energy molecular orbitals dominated by d contributions, which may give rise to a comparatively small energy gap to the lowest unoccupied π orbitals. As will be detailed below, positively charged or potentially positively charged amino acids may exist in a close vicinity to many candidates for hopping transport intermediates. If these amino acids were charged, the energy of nearby excess electrons would decrease, narrowing the energy gap.

For hopping transport involving aromatic amino acids, the effective electronic tunnel splittings can be computed using the methods described in the appendix and above, and one may assume reorganization energies to be close to those typical for charge transfer within proteins. As the X-ray structure is characterized by a resolution too low to assign crystal water, we lack any detailed information about the degree of protonation of acidic and basic amino acids. Thus, little information is available on the value of the driving forces for hopping transfer. Taking into account that ΔG has be smaller than λ to permit an intermediate localization and that $\Delta G > 0$ is likely due to absence of strongly populated intermediate states in UV/vis difference spectra, one may nevertheless deduce an upper and a lower limit for this quantity. These limits can be transferred to the corresponding reaction rates, which are again computed using Marcus's formula, eq 2.2.

We have looked for hopping conduction stepping stones in the capped cylinder models described above. For the transfer N3 → N1b, only a single amino acid, Phe399F (the numbers of the amino acids correspond to the *T. thermophilus* sequence and the single letter to the homologous subunit of the *E. coli* complex I) is sufficiently close to the iron−sulfur clusters, with nonhydrogen edge-to-edge distances of 4.5 and 7.8 Å, respectively. For $\Delta G = 0.47$ eV, transfer rates amount to 240 s^{-1} for transfer from N3 and to 2.2×10^5 s^{-1} for transfer to N1b, which are both compatible with the overall experimental turnover.[22,24,25] For $\Delta G = 0.31$ eV, both rates become equal, $k_{CT} = 5 \times 10^4$ s^{-1}.

For the next transfer in line, N1b → N4, again only a single amino acid, Phe33G, is likely to participate in charge transfer. As above, a ΔG value of roughly half an electron volt (0.51 eV) gives rise to a transfer rate to the aromatic residue, $k_{CT} =$ 160 s^{-1}, that is compatible with the experimental turnover.[22,24,25] $\Delta G = 0.24$ eV leads to equal transfer rates from N1b and to N4, $k_{CT} = 6.5 \times 10^5$ s^{-1}.

A similar situation is encountered for the process N6b → N2. Only Phe100I is sufficiently close to both clusters to participate in hopping transfer. Here, a ΔG of 0.44 eV meets the minimum rate set by experiment, $k_{CT} = 160$ s^{-1}.[22,24,25] For the entire transfer step involving the intermediate amino acid, $k_{CT} = 3.5 \times 10^5$ s^{-1} is the maximum rate achievable by tuning the driving force. In a pictorial way, the results obtained up to this point are summarized in Figure 3.

For the once-presumed bottleneck of the overall charge transfer reaction, N5 → N6a, the situation is more complex, as four aromatic amino acids are candidates for hopping transfer intermediates: Trp247G, His327D, Phe328D, and Tyr42Nqo. Not only may all of them be directly involved in the charge transfer process but electron transfer may also process through more than one intermediate or may include a superexchange component involving one of the four acids.

Looking at the maximum rates achievable by varying the ΔG values, one finds that hopping transport using Tyr42 on subunit Nqo15 (*T. thermophilus* nomenclature) is too slow to be the main stepping stone between the clusters N5 and N6a ($k_{CT} <$ 60 s^{-1}). This is in agreement with the fact that the subunit Nqo15 is only present in complex I originating from *T. thermophilus* and its close relatives.[59] Direct hopping along His327 ($k_{CT} <$ 0.1 s^{-1}) is also too slow to facilitate a sufficiently fast charge transfer.

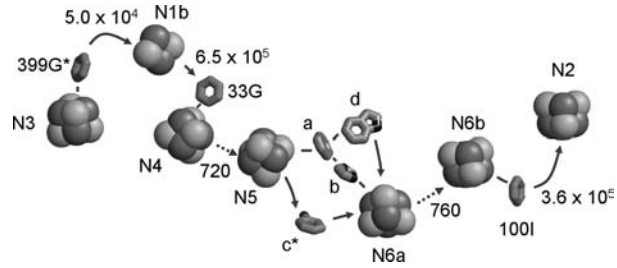

Figure 3. Hopping transfer paths involving aromatic amino acids as stepping stones, as deduced from the rate computations and sequence analysis performed in this work; *a* = Phe328D, *b* = His327D, *c* = Tyr42Nqo15, *d* = Trp42G. Solid arrows: charge transfer involving aromatic amino acid side chains as transiently populated intermediates. Broken arrows: direct intercluster charge transfer. Charge transfer rates are given in s^{-1}. For processes involving aromatic amino acids, upper limits of the total cluster-to-cluster rates are given.

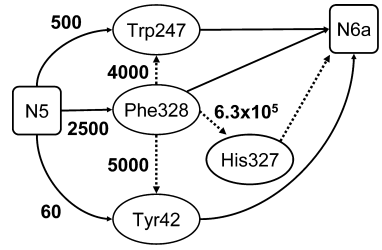

Figure 4. Potential charge transfer paths for the process N5 → N6a involving aromatic amino acids. Solid arrows: charge transfer involving a single aromatic amino acid. Broken arrows: charge transfer involving two aromatic amino acids. The numbers correspond to the maximum reaction rates in s^{-1}.

The five indirect paths, N5 → Trp247 → N6a (a), N5 → Phe328 → N6a (b), N5 → Phe328 → His327 → N6a (c), N5 → Phe328 → Tyr42 → N6a (d), and N5 → Phe328 → Trp247 → N6a (e), are all compatible with the experimentally observed total turnover. They are illustrated in Figure 4. We note that for the first of these paths, superexchange involving Phe328D plays an important role. It speeds up the CT rate by almost 1 order of magnitude and brings it into the experimental range. Thus, in any of these cases, Phe328D is central to CT between the two Fe/S clusters that exhibit the largest intercluster separation, and it is an excellent candidate for studying the kinetics of variants. As Phe328D protrudes from the NuoD subunit geometry and may be interpreted as a hydrophobic anchor, particular care should be devoted to ensure that its nonaromatic substituent leaves the structure of the mutant protein intact.

In connection with the five hopping paths (a−e) discussed above, one mutation experiment already performed may help to further untie the Gordian knot of charge transfer from N5 to N6a. The 327HisDAla mutant exhibits a turnover of roughly one-half as compared to the wild type.[60] This finding can be rationalized within one of the following three scenarios: First,

(59) Pohl, T.; Walter, J.; Stople, S.; Defeu Soufo, H. J.; Graumann, P. L.; Friedrich, T. *BMC Biochem.* **2007**, *8*, 13.
(60) Kashani-Poor, N.; Zwicker, K.; Kerscher, S.; Brandt, U. *J. Biol. Chem.* **2001**, *276*, 24082–24087.

c is not rate limiting in the wild type, whereas hopping from N5 to N6b becomes the kinetic bottleneck for the variant, now following a different hopping path. Inspecting the large difference in the rates in the absence and in the presence of 327HisD, we consider this scenario to be the likeliest. Second, c may be rate limiting in the wild type, and one of the different N5 → N6a charge transfer paths discussed above may half the reaction rate for the mutant. Third, lacking any knowledge about the local structure of the mutant, one cannot exclude that 327HisD may support a local geometry favorable for charge transfer, which 327AlaD may lack.

3.3. Multiple Sequence Alignment. With the possibility of aromatic amino acids participating as essential stepping stones for charge transfer processes, we had a look at the sequence of available complex I homologues. This concerns sequences around the amino acids presumed to participate in the steps N3 → N1b, N1b → N4, N6b → N2, and N5 → N6a. We have made an attempt to cover a broad spectrum of prokaryotes and eukaryotes including simple invertebrates, fungi, and mammals. Alignments have been performed using the ClustalX program[61−63] with parameters as given in the footnote.[64] Protein sequences have been taken from the NCBI database, and the results have been visualized making use of the Seaview program.[65] In the following, the amino acid index always refers to *Thermus thermophilus*.

We illustrate the alignment for the charge transfer reaction N1b → N4, for which we have strong theoretical evidence that Phe33G acts as an intermediate within a hopping process. The result is shown in Table 3. Phe33G is conserved with the exception of *Neurospora crassa*, where it is replaced by another aromatic amino acid, viz., a tyrosine that may support hopping transport in a similar manner. In most of the organisms listed in Table 3, Phe33G is accompanied by an amino acid that can be protonated (arginine or histidine) in position 32. A positive charge in the direct vicinity of a hopping electron stabilizes the excess charge and may lower the corresponding amino acid side chain orbitals to be accessible for a transient, nonvirtual population. We note that most other organisms exhibit other aromatic amino acids close to the position 33, which may help to transfer electrons via different paths or by assisting hopping transfer via a superexchange component, as discussed above.

We now turn to the amino acids that were identified as candidates for supporting charge transfer between the clusters N5 and N6a. Phe328D is conserved, whereas His327D is replaced by a serine in *A. fulgidus*. Trp247G is conserved, apart from *S. coelicolor*, where it is replaced by phenylalanine. As the next nearest neighbor to the left of Trp247G, we find almost exclusively arginine as a positively charged amino acid.

At the postion of Phe100I, which may participate in charge transfer between the clusters N6b and N2, aromaticity is predominantly conserved, and we encounter either phenylalanine or tyrosine. Again, *S. coelicolor* is an exception, and we find a leucine replacing the aromatic amino acid. The entire region around Phe100I is strongly conserved, which is not suprising considering the fact that it contains cysteines at the positions 98, 101, and 104 that act as ligands to the cluster N6b. As a reoccurring theme, arginine or lysine are found in the close vicinity (position 97) of the aromatic amino acid under review.

Of all aromatic amino acids that were identified as candidates for a simple hopping transfer involving a single stepping stone, only Phe399F is not fully conserved even within the group of prokaryotes. Nevertheless, aromatic amino acids very frequently occur in positions 397 or 398. Whether they actually participate in hopping transfer will be an interesting question for future studies, which at present still lack the geometrical basis stemming from X-ray structures of the corresponding proteins.

Table 3. Multiple Sequence Alignment around Phe33 (NuoG subunit)

	*
Homo sapiens	QACEKVGMQIPRFCYHERLSVAGNC
Danio rerio	QACEKVGVQIPRFCYHDRLSVAGNC
Caenorhabditis elegans	QACALVGVDIPRFCYHDRLSIAGNC
Arabidopsis thaliana	QACEVAGVDIPRFCYHSRLSIAGNC
Acanthamoeba castellanii	QACLKNKVDISRFCFHEKLSIAGNC
Neurospora crassa	QACEKAGVTIPRYCYHEKLMIAGNC
Salinibacter ruber	QFCLNQGIELPHFCYHPAMSIPANC
Streptomyces coelicolor	RAAEQLGIEIPRFCDHPLLDPAGAC
Rhodobacter sphaeroides	TTCLSAGIEIPHFCWHGDLGSVGAC
Escherichia coli	EACLSLGLDIPYFCWHPALGSVGAC
Thermus thermophilus	DAVFHAGYDVPLFCSEKHLSPIGAC
	. .
	30 40

4. Conclusions

In this work, we have presented an atomistic view of charge transfer in the respiratory chain complex I. A carefully parametrized tight-binding Hamiltonian has been supplemented by a Hubbard-like repulsion term to account for d orbital electron−electron interaction and a reaction field that mimics polarization effects. With a recently published X-ray analysis of the protein and its cofactors as a geometrical basis, we have been able to obtain a theoretical view that is neither biased a priori toward any particular reaction mechanism nor requires an artificial partitioning of the protein into donor, acceptor, and bridge regions. As crucial energetic quantities of Marcus's theory of charge transfer, the effective electronic couplings between iron−sulfur clusters, the entities hitherto assumed to be the only centers of electron localization within the protein, have been computed. In connection with experimental driving forces, we find intercluster charge transfer rates that are by far too small even compared to moderate experimentally observed total turnover rates. This statement holds for through-space, through-bond, and superexchange charge transfer involving subsets of the protein that contain more than 10^3 atoms. This

(61) Higgins, D. G.; Bleasby, A. J.; Fuchs, R. *CABIOS, Comput. Appl. Biosci.* **1992**, *8*, 189–191.
(62) Thompson, J. D.; Higgins, D. G.; Gibson, T. J. *Nucleic Acids Res.* **1994**, *22*, 4673–4680.
(63) Thompson, J. D.; Gibson, T. J.; Plewniak, F.; Jeanmougin, F.; Higgins, D. G. *Nucleic Acids Res.* **1997**, *24*, 4876–4882.
(64) The following options have been used: slow pairwise alignment, blosum series protein weight matrix, 10.00 gap opening penalty, 0.10 gap extension penalty, gap separation distance 4, end gap separation penalty OFF, residue specific penalties ON, hydrophilic gap penalties ON, hydrophilic residues GPSNDQEKR, delay divergent sequences 30.
(65) Galtier, N.; Gouy, M.; Gautier, C. *CABIOS, Comput. Appl. Biosci.* **1996**, *12*, 543–548.
(66) Nakamaru-Ogiso, E.; Matsuno-Yagi, A.; Yoshikawa, S.; Yagi, T.; Ohnishi, T. *J. Biol. Chem.* **2008**, *283*, 25979–25987.

negative result does not depend significantly on the details of the electronic structure model, such as the type of the long-range coupling or the numerical procedures used to compute the t_{DA} values.

This picture is changed once aromatic amino acid side chains are considered as stepping stones within a hopping mechanism. Here, for reasonable values of the driving force $0 \leq \Delta G \leq 0.5$ eV with reference to the Fe/S clusters, transfer rates in accord with the experiments have been computed. From our perspective, and at variance to deductions from a simple through-space mechanism, the presence of all Fe/S clusters depicted in Figure 5 is crucial for the observation of electron transfer with a rate that is at least on the order of 160 s^{-1}. The reaction steps N3 to N1b, N1b to N4, and N6b to N2 involve a phenylalanine, and for the transfer from N5 N6a, four aromatic amino acids have been identified as candidates for transient charge localization. Regardless of the details of the mechanism for this step, a phenylalanine again plays a central role. Here, our model also helps to rationalize a recent mutation experiment, His327DAla. According to our calculations, the CT steps N4 to N5 and N6a and N6b still obey a simple intercluster transfer mechanism that lacks temporary charge localization on intermediates.

A muliple sequence alignment reveals that all phenylalanines identified as participants in charge transfer events are conserved within all complex I homologues with the exception of Phe399F possibly involved in the charge transfer between N3 and N1b. The function of this amino acid is likely to have been taken over by other nearby aromatic amino acids that show up in all other genomes taken into account in our studies. Frequently, phenylalanine is accompanied by a neighboring amino acid with a positive charge that may lower the vacant aromatic orbitals to be more easily populated by excess electrons.

Using the *E. coli* complex I as a model, we have started to mutate the positions of the aromatic amino acids identified to participate in charge transfer. Preliminary results suggest that all mutations introduced had an effect on the overall electron transfer rate of the complex from NADH to ubiquinone.

In summary, we hope to have made a case to consider the amino acids in complex I not just as a scaffold supporting the cofactors or as an effective, homogeneous medium to be experienced by tunnel processes but as an important, differentiated element of the electronic structure and of charge transfer processes. This view can be verified or falsified with the help of mutation experiments on the aromatic amino acids shown in Figure 6 or by looking for spectroscopic fingerprints of phenylalanine radical anions via IR or UV/vis difference spectroscopy.

Acknowledgment. It is a pleasure to thank L. Cederbaum, K. Dörner, P. Hildebrandt, and P. Tavan for fruitful discussions and T. Pohl for his kind help with the sequence alignments.

Supporting Information Available: An appendix describing the electronic structure model and its parametrization and multiple sequence alignments around the amino acid (i) Phe399 (NuoF subunit), (ii) His327 and Phe328 (NuoD subunit), (iii) Trp247 (NuoG subunit), and (iv) Phe100 (NuoI subunit). This material is available free of charge via the Internet at http://pubs.acs.org.

JA900352T